Progress in Organic Coatings 127 (2019) 300–307

Contents lists available at ScienceDirect

Progress in Organic Coatings

journal homepage: www.elsevier.com/locate/porgcoat

Corrosion inhibition enhancement of Al alloy by graphene oxide coating in NaCl solution

Rasoul Ranjandish Laleh, Hadi Savaloni*, Fateme Abdi, Yaser Abdi

School of Physics, College of Science, University of Tehran, Tehran, Iran

ARTICLE INFO

Keywords:
Graphene oxide
Aluminum
Corrosion
Electrochemical impedance spectroscopy
Equivalent circuit

ABSTRACT

In this work the influence of graphene oxide (GO) coating on the corrosion inhibition of Al substrates (7049 alloy with fifteen elements) in 0.6 M NaCl solution is reported. According to the Raman spectroscopy results GO was formed on the Al. Surface morphology of both untreated Al and the GO coated Al (GO/Al) sample was studied by atomic force microscope (AFM). AFM results showed that by coating the Al alloy surface with GO, the surface becomes smoother and the needle like surface structure of Al changes to strains/lines of grains with valleys between them. Corrosion resistance of the samples was studied by the electrochemical impedance spectroscopy (EIS) which showed a great enhancement in the corrosion resistance of GO/Al sample relative to that of untreated Al (1237 times). The equivalent circuit for GO/Al sample, using the EIS data showed omission of inductance element that obtained for the untreated Al sample. Further investigation on obtaining relationship between corrosion inhibition and equivalent circuit elements was carried out.

1. Introduction

Aluminium and its alloys are used in excess in different industries due to their lightness, sheer strength, electrical and high thermal conductivity and corrosion resistance [1,2]. However, their use is limited because of their low hardness and low resistance. When the surface of Al is exposed to the atmosphere a thin oxide layer forms on the surface which in fact protects it from further oxidation and also enhances its corrosion resistance. However, when metals and in particular Al is exposed to a polar environment/solvent (water or alcohol) or electrolyte solution (salt, acid or alkali dissolved in water) the surface of metal acquires electric potential because water polar molecules have a negative extra charge on the oxygen atom and a positive charge on the hydrogen atoms, electric forces from water molecules and metal atoms force the metallic ions to leave the metal and move towards the solution as cations. This process is the mechanism of corrosion of a metal in the presence of an electrolyte such as sea water.

The corrosion process is the interaction between a material, usually a metal, and its environment that results in deterioration of the material [3]. Hence, protection of metal surface from corrosion in different environments is of prime importance which may be achieved by different coatings on the surface or surface modification using different methods [4–6].

In recent years the researchers in the field of material science have been attracted towards the use of graphene [7–11] as a coating candidate for corrosion inhibition of metals/materials because of its high corrosion resistance which is due to strong coupling of carbon atoms in two dimensional configurations that in turn makes it chemically inert and thermally stable [12]. On the other hand, defect free graphene monolayer is non-penetrable material for gases and liquids [13]. It also shows high resistance against aggressive acids such as HF and aggressive anions such as chloride, Cl^- [14]. Perhaps the most important property of graphene is that it transmits 97% of the incident visible light [15]. This means that only a few atomic layer of graphene not only can retain the original appearance of the object but also can enhance its corrosion resistance remarkably. However, it is worthwhile to mention that production of defect free graphene in large sizes for industrial applications is a nontrivial and almost impossible task. Therefore, one should seek a more achievable alternative. Different researchers have shown that graphene oxide (GO) may be the best candidate because of the strong interaction between metal surface and GO [16–18]. In addition, apart having two dimensional graphene plane structure, functional groups such as epoxies and hydroxyls are also attached to these planes which give additional super features to graphene [19].

Graphene oxide (GO) is used as a protective coating to inhibit the corrosion of aluminum current collector used in lithium ion batteries [20]. Dedkov et al. [21] reported that GO with a range of reactive oxygen functional groups (polar in nature) can behave as negative

* Corresponding author.
E-mail address: savaloni@khayam.ut.ac.ir (H. Savaloni).

https://doi.org/10.1016/j.porgcoat.2018.11.031
Received 25 August 2017; Received in revised form 4 June 2018; Accepted 24 November 2018

Table 1
Chemical composition of Al (7049) used in this work.

Element (wt%)													
Ti	Ga	P	Mn	Ca	K	Cl	S	Fe	Si	Cr	Cu	Mg	Zn
0.050	0.015	0.014	0.040	0.029	0.017	0.035	0.10	0.22	0.23	0.31	2.1	4.1	8.2

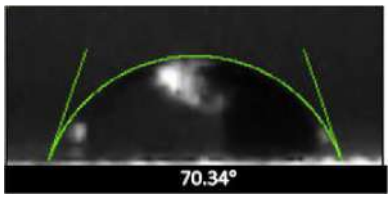

Fig. 1. Contact angle for a 10 mg distilled water on polished surface of Al.

charged species when exposed to an electrolyte (e.g., NaCl in this work). Hence, the electrostatic repulsion between the negative charges on GO and electrolyte anions (e.g.Cl^- in this work) can impede the access of the anions responsible for pitting corrosion to a metal surface. All of the above mentioned properties of graphene oxide provide suitable condition for its use in the field of corrosion inhibition of metals.

In this work we have used GO coating on Al alloy to investigate the degree of enhancement of corrosion inhibition of this alloy in 0.6 M NaCl solution. GO was synthesized using the modified Hummers method [18], then using the lift up method, GO was lifted by Al sample from the solution and dried in an oven. Hence, Al was covered with GO. Raman spectroscopy showed the proper formation of GO on Al alloy (7049 with fifteen elements in its composition). Electrochemical impedance spectroscopy (EIS) test was carried out on uncoated and GO coated Al samples in 0.6 M NaCl solution that is considered in the literature as corresponding to the sea water NaCl concentration. Different corrosion parameters were obtained from the simulated equivalent circuits for the EIS results.

2. Experimental details

Commercial aluminum alloy as received (7049 with fifteen elements in its composition) with 3 mm thickness were prepared in 20×20 mm^2 dimensions. The X-ray fluorescence (XRF) method (Philips PW2404) was used to determine the composition of Al and data is given in Table 1. The surface of Al samples were polished using emery papers grades 600, 800, 1500, 3000 and 5000, respectively. After thorough cleaning of the samples in ultrasonic bath with heated acetone then ethanol, they were coated with graphene oxide using the lift up method; graphene oxide was lifted by Al sample from the solution and dried in an oven. This method is almost the same as that mentioned by Lin et al. [22] as immersion and subsequent thermal treatment for obtaining good adhesion of GO sheet on metals. This can be either due to the existence of large amount of oxygen functional groups in a 2D GO sheet which has strong adhesion to the hydrophilic surface [23] or due to the chemical interaction between metal and GO sheets (metal and metal ions can chemically bond with GO sheets) [24–26] where the positive charge on the metal surface promotes the formation of the interaction. In addition, many researchers have reported that hydrophobicity strongly depends on the surface roughness [e.g., 27]. The AFM measurement resulted in a surface roughness value of 10.76 nm for the Al samples after polishing which indicates low surface roughness. Hence, it can be assumed as hydrophilic surface. However, using the procedure described in [27] a contact angle of 70.34° was obtained, for a droplet of distilled water (10 mg) on the polished Al substrate (Fig. 1) which confirms the hydrophilic behavior of Al surface used in this work. This result agrees well with Moon et al.'s results [23]: GO sheet has strong adhesion to the hydrophilic surface.

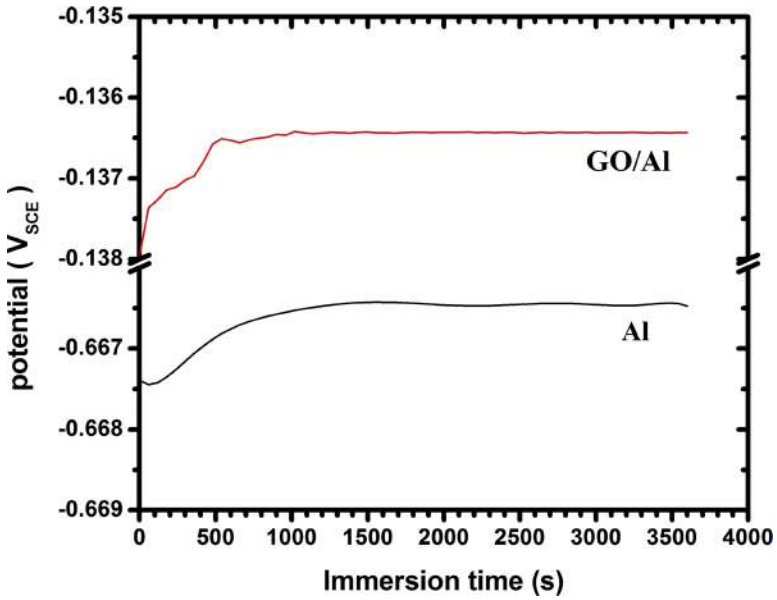

Fig. 2. The obtained OCP values for the bare Al and GO coated Al.

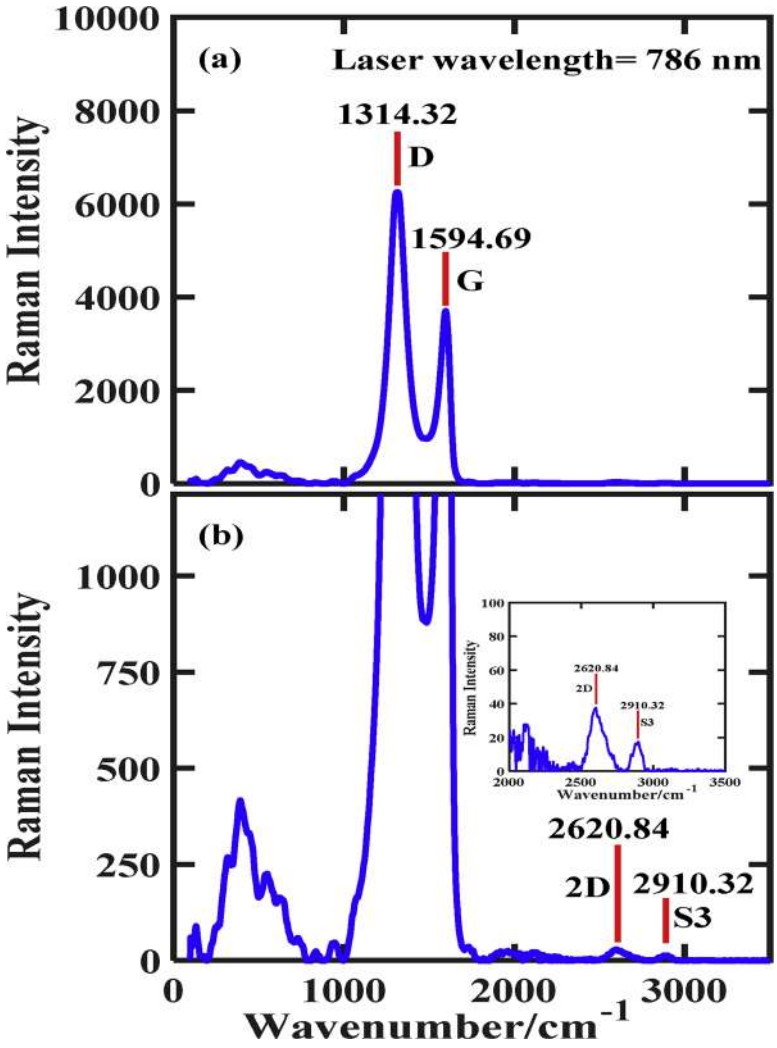

Fig. 3. Raman spectrum of Al alloy (7049) coated with graphene oxide. a) shows the high intensity peaks and b) shows the low intensity peaks.

Graphene oxide was synthesized using the modified Hummers method [18]. In this method 2 g of graphite powder, 1 g of $NaNO_3$ and 46 ml of H_2SO_4 were mixed together, then the mixture was placed in an ice bath until its temperature reduced to 10 °C. In the next step, 6 g of $KMnO_4$ was slowly added to the mixture so that the temperature of the solution did not rise above 20 °C. The resulted solution was kept in a fixed temperature of 35 °C for 12 h, then 92 ml of de-ionized water was slowly added to the solution and 340 ml of H_2O_2 was added to the obtained solution. Finally the solution was filtered using a suitable filter. The filtered sediment was washed with de-ionized water and HCl periodically so that no trace of acid remained in the remaining sediment. The obtained dough was dried at 65 °C for 24 h. 0.1 g of the resulted graphite oxide was dispersed in 50 ml of de-ionized water and was well stirred for 3 h, then the obtained solution was placed in an ultrasonic bath for 2 h. In the last stage the graphene oxide solution was placed in a fixed place for 48 h so that no movement occurs in it.

Thickness of the prepared GO sheet depends on the exfoliation step in the mentioned Hummer's method. In the method used in this work the thickness of the obtained GO sheets varied between 1–4 nm corresponding to 1–5 GO layer. The GO thickness is estimated from the height profile of selected line(s) of selected area(s) of AFM images.

Surface physical morphology/nanostructure and roughness of the samples was obtained by means of AFM (Nt-mdt scanning probe microscope, BL022, Russia; with low stress silicon nitride tip of less than 200 Å radius and tip opening of 18°) and FESEM (Hitachi S-4100 SEM, Japan) analysis. Root mean square (rms) and average surface roughness as well as average grain size of the samples were obtained from the 2D AFM images using Nova and JMicroVision softwares, respectively. Several samples were used in all analysis to guarantee reproducibility of the results.

Electrochemical impedance spectroscopy (EIS) was performed using a potentiostat coupled to PC (Ivium, De Zaale 11, 5612 A J Eindhoven, Netherlands) with reference to the open circuit potential (OCP) (Fig. 2) and in the frequency range of 100 KHz to 0.01 Hz with a voltage amplitude of 0.01 V with respect to the open circuit potential. The open circuit potential was monitored for 1 h to obtain three electrode cell stability before performing electrochemical test. The analysis of the impedance spectra was performed using Zsim software and the equivalent circuit fitted to the experimental data was obtained.

All measurements were performed at 298 K. An initial delay of one hour for the samples to reach a steady state condition was considered before electrochemical impedance spectroscopy (EIS) test.

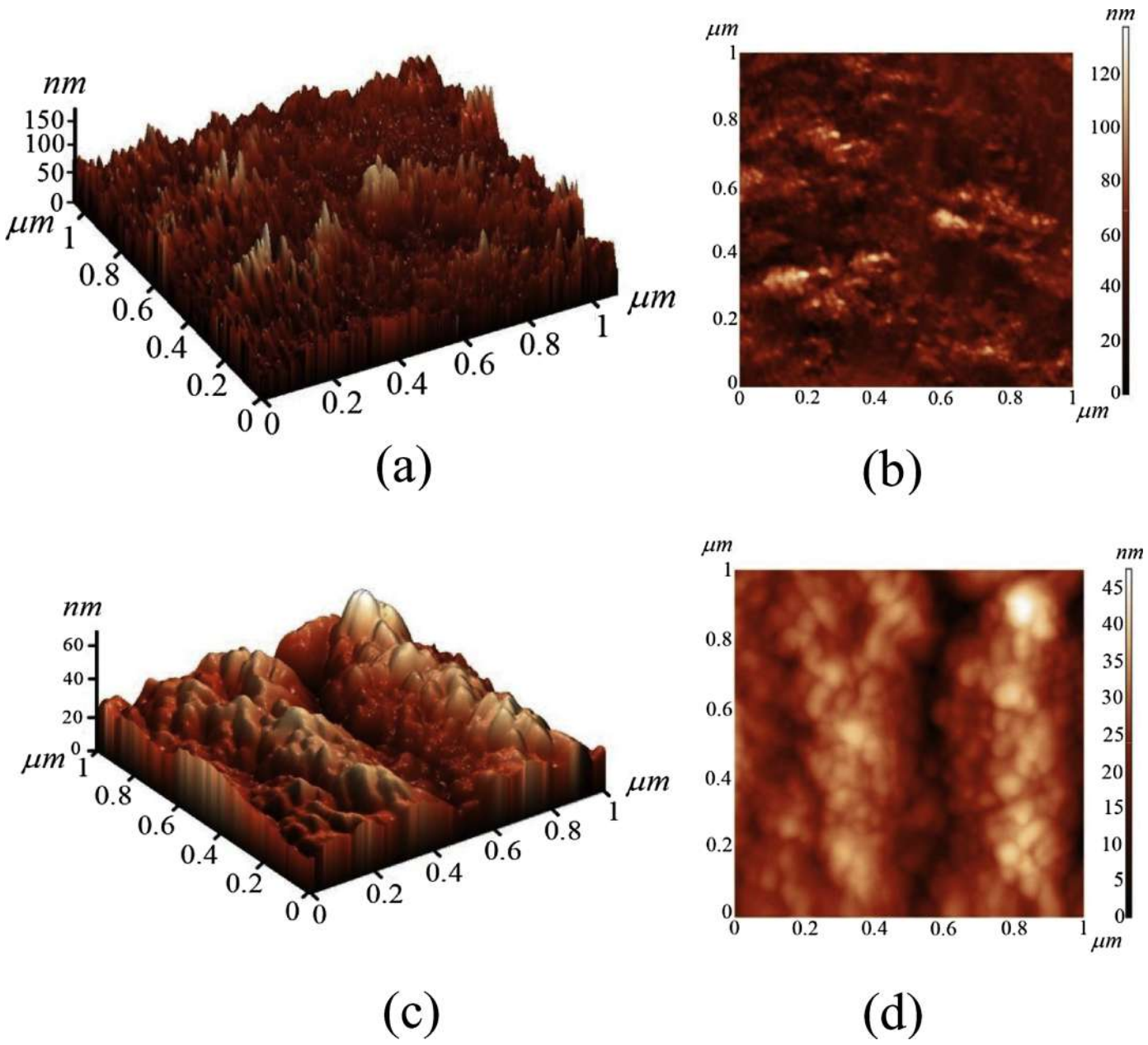

Fig. 4. 2D and 3D AFM images of; a, b) untreated Al alloy (7049) samples, c, d) Al alloy (7049) samples coated with graphene oxide.

Table 2
Average and Root mean square surface roughness obtained from AFM analyses.

Sample	R_{ave} (nm)	R_{rms} (nm)
Al	10.76	14.38
GO/Al	5.51	6.9

In order to carry out this analysis only an area of 1 cm^2 was exposed to the 0.6 M NaCl corroding medium. The samples (working electrode) were mounted in an inert fixture (polyamide). This allowed an electrical contact to be supplied to the sample, without being influenced by undesirable effects on the working electrode. A saturated calomel electrode was used as a reference electrode and a platinum electrode used as auxiliary one.

The Raman spectroscopy of the samples was carried out using the (SENTERRA 2009 spectrometer, Germany) that uses a laser with 785 nm wavelength.

3. Results and discussion

3.1. Raman spectroscopy

Raman spectroscopy is a non-destructive technique that is widely used to obtain structural information about carbon based materials [28]. The Raman spectrum of graphene oxide on Al sample (GO/Al) is given in Fig. 3 which confirms the formation of GO on Al. Two peaks can clearly be observed (Fig. 3(a)) at 1314.32 cm^{-1} (D band) and

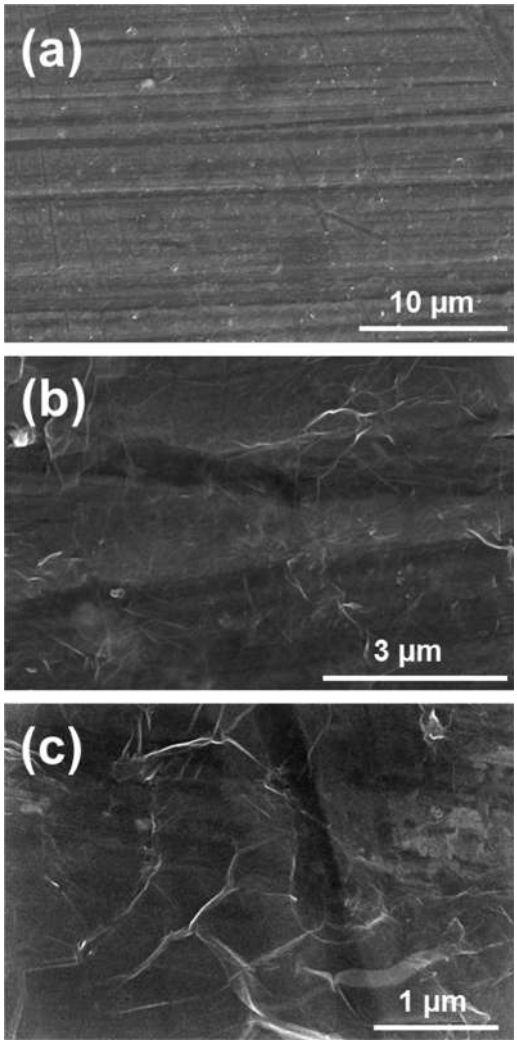

Fig. 5. FESEM images of the surface of Al alloy (7049) samples coated with graphene oxide.

1594.69 cm^{-1} (G band) characteristics of structural imperfections created by the attachment of oxygenated groups on the carbon based plane and all sp^2–hybridized carbon networks, originated from the first order scattering from the doubly degenerate E_{2g} phonon modes of graphite in the Brillouin zone center, respectively [29–32]. It should be mentioned that the position of the D peak depends on the energy of the laser used. Higher the energy of the laser the higher Raman shift for the D peak is observed [33]. In addition, the G peak also shifts towards red wavelengths by increasing the number of layers in the structure of GO [34]. The 2D peak (Fig. 3(b)) at 2620.84 cm^{-1} is a second order peak which appears as a result of zone boundary phonons. Because zone boundary phonons do not satisfy the Raman fundamental selection rules, they are observed only in resonant conditions. The low intensity of the 2D band in the spectra in Fig. 3 indicates the high number of defects in the graphene coating, while combination of the D and G peaks leads to an S3 peak at higher wavenumber of about 2910.32 cm^{-1}.

3.2. AFM and FESEM

The surface morphology of Al and GO/Al samples were analyzed by AFM. In Fig. 4 the 2D and 3D AFM images of the untreated Al and GO/Al samples are given. AFM images of untreated Al sample (Fig. 4(a and b)) show very small needle-like grain structures which are patched at different areas of the surface and may indicate the bimodal distribution of grains on the surface of the Al sample (see 2D image of this sample) while after coating with GO (Fig. 4 (c and d)) larger grains are formed with deep valleys between strains/lines of grains. Covering of the needle-like patches of the untreated sample by GO should have filled/covered the very small gaps between the needle-like grains and smoothed these areas of the surface of the sample, while between these areas groove like valleys are formed.

Average (R_{ave}) and root mean square (R_{rms}) surface roughness results obtained from the AFM measurements for both untreated Al and the GO/Al samples are given in Table 2. It can be seen that the surface roughness is decreased when Al is coated with GO which can be the result of the procedure mentioned above.

Fig. 5 shows different scale FESEM surface images of Al coated with graphene oxide. Al surface scratches/grooves remained from polishing process and wrinkles/kinks of graphene oxide can also be observed on these images.

3.3. Electrochemical impedance spectroscopy

Results of electrochemical impedance spectroscopy (EIS) analysis of the untreated Al sample and the GO/Al sample are given in Fig. 6. In Fig. 6(a–c) the Nyquist plots, Bode and phase diagrams are given, respectively. These plots can be related to the simulated equivalent circuits and the components of the equivalent circuits are indicative of the physical, chemical or electrochemical process(s) in the corroding environment. It can be observed that the GO/Al sample show much better corrosion behavior than the untreated sample.

In Fig. 6 the Nyquist plot of the untreated Al sample consists of two semi-circles each of which are in different direction with respect to Z' axis and are also formed above and below the zero value of –Z" axis. The first semi-circle which is above zero axis of –Z" (which occurs at higher frequencies) is indicative of capacitance behavior of the sample (as a result of positive phase difference of 90° between current and voltage), hence an *RC* circuit should explain this behavior with a constant phase element called double layer capacitor CPE_{dl} with an impedance (charge transfer resistance) R_{ct} [35]. The double layer capacitor is related to the interface between the metal and the solution (NaCl) and is formed by the ions adsorbed on the metal electrode surface, so that the charged metal electrode is separated from metallic ions by an insulating space of a few angstroms. The value of this double layer capacitor depends on several factors such as potential of the electrode, temperature, ionic density of the electrolyte solution, type of ions, and surface adsorption of impurities. The second semi-circle which is below zero axis of –Z" (which occurs at lower frequencies) is indicative of inductance behavior of the sample (as a result of negative phase difference of 90° between current and voltage) R_L at low frequencies. The appearance of constant phase element semi-circle before the inductance semi-circle is due to its smaller time constant. The equivalent electric circuit for the untreated Al sample is given in Fig. 7(a).

Interpretation of inductance behavior in the EIS spectrum is one of the most difficult problems for corrosion systems. However, it is believed that the inductive loop observed is associated with the weakening of the protective effectiveness of the aluminum oxide layer due to the anodic dissolution of aluminum alloy [36].

Further and more careful analyses of the results may be achieved from the Bode and phase diagrams which can be obtained from the best

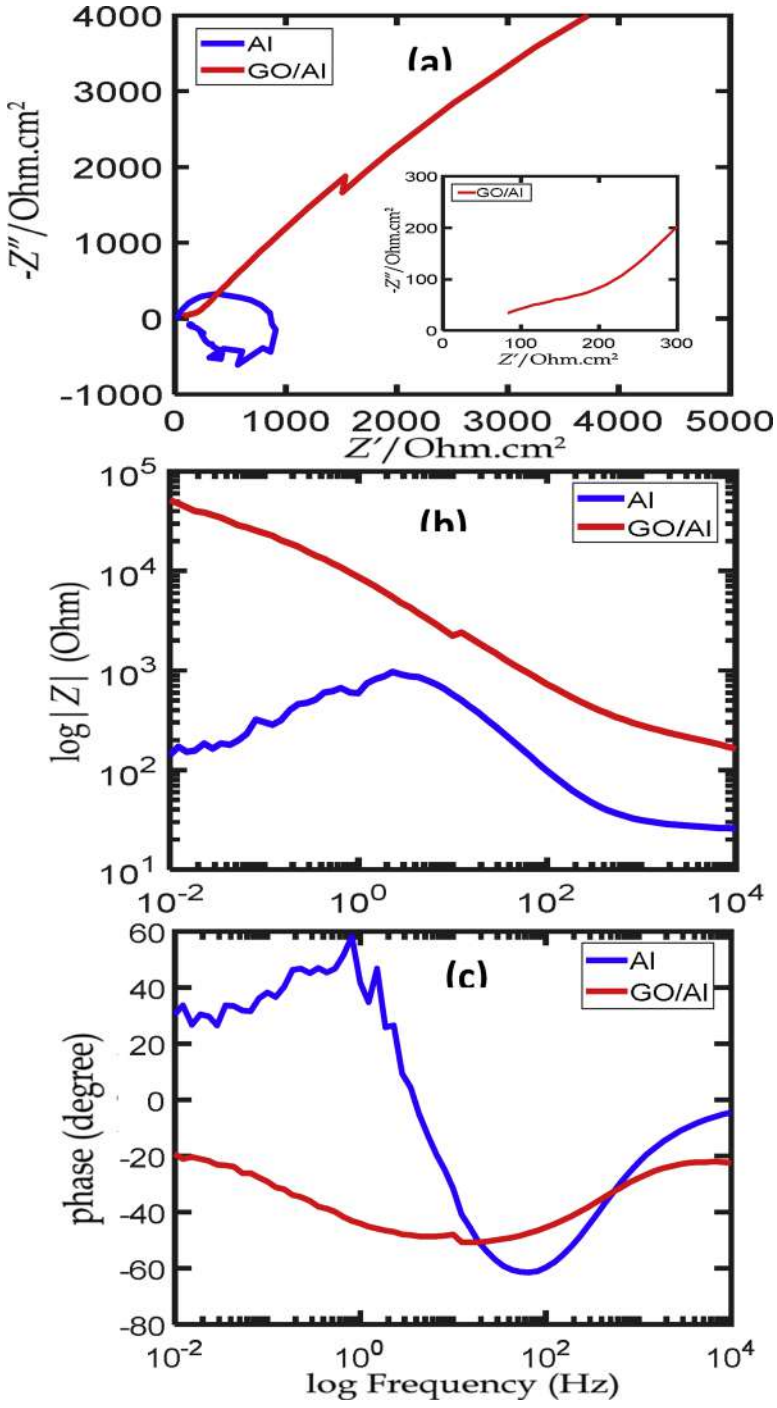

Fig. 6. a, b and c) Experimental Nyquist, Bode and phase diagrams for Al, and Al coated with graphene oxide samples, respectively.

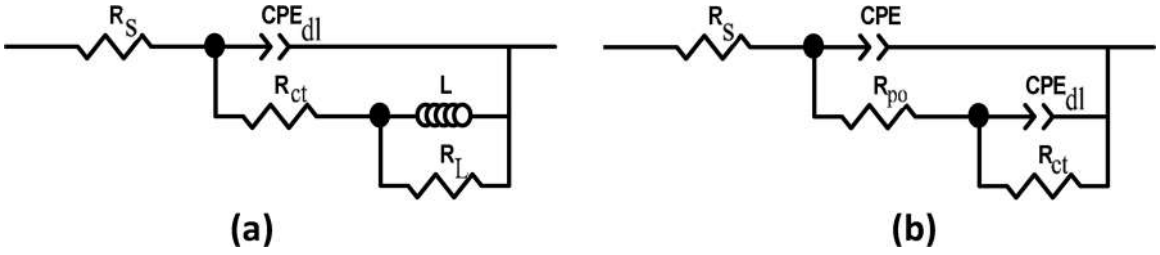

Fig. 7. Electrical equivalent circuits of; a) untreated Al alloy (7049) and, b) graphene oxide coated Al alloy (7049) samples.

Table 3
Electrochemical parameters of Al (7049) and GO/Al samples subjected to corrosion test in 0.6 M NaCl, obtained from the simulation procedure using the Zsimsoftware.

GO/Al	Al	
34.9	26.5	R_s (Ω. cm^2)
14×10^{-6}	34.5×10^{-6}	CPE_{dl} (F. cm^{-2})
0.68	0.88	n
61860	50	R_{ct} (Ω. cm^2)
25×10^{-6}	–	CPE (F. cm^{-2})
0.47	–	n
274	–	R_{po}(Ω. cm^2)
–	100	L (H. cm^2)
–	900	R_L (Ω. cm^2)

fit procedure between experimental and the equivalent circuit.

The Bode diagram of the untreated Al sample in Fig. 6(b) shows that at high frequencies the impedance is almost constant while the phase diagram of this sample (Fig. 6(c)) at high frequencies decreases. These results are indicative of a resistance response and show that a resistance due to presence of electrolyte solution (i.e., NaCl solution) is acting on the system as R_s.

The Nyquist plot of GO/Al sample (Fig. 6(a)) shows two semi-circles above the zero axis of –Z". The first semi-circle has a very small radius and does not reside on the horizontal axis. These characteristics can be related to the deviation of ideal capacitor behavior and assigned as constant phase element and we show it by CPE. The equivalent electric circuit for the GO/Al samples can be designed as shown in Fig. 7(b). The electrolyte resistance is represented by R_s, the metal/electrolyte interface is represented by a capacitance CPE_{dl}, and a resistance (charge transferred resistance) R_{ct}, while the surface coating is represented by a constant phase element CPE and a pore resistance R_{po}.

In Table 3 the quantities obtained from the fitting of equivalent circuits of Fig. 7 to the experimental results are given. These values are obtained using the simulation procedure by the aim of Zsim software. These results show that by coating of Al with GO the inductance values of the equivalent circuit (Fig. 7(a)) disappeared while the charge transfer resistor R_{ct}, increased relative to the untreated Al. In Fig. 8 results of fitting procedure to the experimental data (Nyquist plots) clearly confirm this analysis.

4. Conclusion

Graphene oxide was prepared using Hummers's method and used as a coating for the Al (7049 alloy with fifteen elements) surface. AFM analysis of the surface of untreated Al and GO coated Al (GO/Al) showed improvement of the surface roughness of Al after GO coating by a factor of 2. The EIS and the results of simulation for the equivalent circuits showed an inductance element for the untreated Al which was disappeared after GO coating of the Al sample. A high degree of corrosion enhancement (a factor of 1237 times) was achieved for GO coated Al sample relative to the untreated Al.

Acknowledgements

This work was carried out with the support of the University of Tehran. HS is grateful to the Centre of Excellence for Physics and technology of quantum devices, Department of Physics, University of Tehran for partial support of this work.

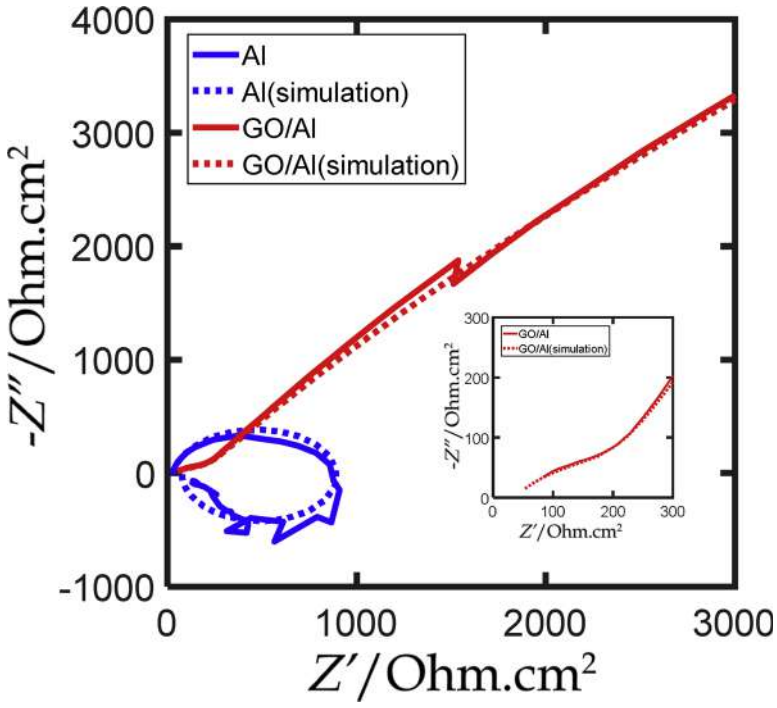

Fig. 8. Nyquist diagrams of untreated Al alloy (7049) and graphene oxide coated Al alloy (7049). (Solid line) experimental; (dashed line) simulation.

References

[1] E.A. Starke, J.T. Staley, Application of modern aluminum alloys to aircraft, Prog. Aerosp. Sci. 32 (1996) 31–172.
[2] P.K. Rohatgi, Aluminum alloy-fly ash composite (Ashalloy)–future foundry products for automotive applications, Fuel Energy Abstr. 39 (1998) 25-25.
[3] A. Groysman, Springer science & business media, Corrosion for Everybody, (2009).
[4] X. Nie, E.I. Meletis, J.C. Jiang, A. Leyland, A.L. Yerokhin, A. Matthews, Abrasive wear/corrosion properties and TEM analysis of Al_2O_3 coatings fabricated using plasma electrolysis, Surf. Coat. Technol. 149 (2002) 245–251.
[5] A. Frignani, F. Zucchi, G. Trabanelli, V. Grassi, Protective action towards aluminum corrosion by silanes with a long aliphatic chain, Corros. Sci. 48 (2006) 2258–2273.
[6] L. Tong, F. Zhang, C. Xue, L. Li, Y. Yin, Structure stability and corrosion resistance of nano-TiO2 coatings on aluminum in seawater by a vacuum dip-coating method, Surf. Coat. Technol. 205 (2010) 2335–2339.
[7] P. Dhiraj, J.C. Tuberquia, R.R. Harl, G.K. Jennings, K.I. Bolotin, Graphene: corrosion-inhibiting coating, ACS Nano 6 (2012) 1102–1108.
[8] R.K.S. Raman, A. Tiwari, Graphene: the thinnest known coating for corrosion protection, J. Miner. Met. Mater. Soc. (Jom) 66 (2014) 637–642.
[9] R.K.S. Raman, P.C. Banerjee, D.E. Lobo, H. Gullapalli, M. Sumandasa, A. Kumar, et al., Protecting copper from electrochemical degradation by graphene coating, Carbon 50 (2012) 4040–4045.
[10] N.T. Kirkland, T. Schiller, N. Medhekar, N. Birbilis, Exploring graphene as a corrosion protection barrier, Corros. Sci. 56 (2012) 1–4.
[11] S.S. Chandra, A.K. Samantara, M. Seth, S. Parwaiz, B.P. Singh, P.C. Rath, et al., A facile electrochemical approach for development of highly corrosion protective coatings using graphene nanosheets, Electrochem. commun. 32 (2013) 22–26.
[12] J. De-en, B.G. Sumpter, S. Dai, How do aryl groups attach to a graphene sheet? J. Phys. Chem. B 110 (2006) 23628–23632.
[13] B.J. Scott, S.S. Verbridge, J.S. Alden, A.M. Van Der Zande, J.M. Parpia, H.G. Craighead, et al., Impermeable atomic membranes from graphene sheets, Nano Lett. 8 (2008) 2458–2462.
[14] E. Stolyarova, D. Stolyarov, K. Bolotin, S. Ryu, L. Liu, K.T. Rim, et al., Observation of graphene bubbles and effective mass transport under graphene films, Nano Lett. 9 (2008) 332–337.
[15] R.R. Nair, P. Blake, A.N. Grigorenko, K.S. Novoselov, T.J. Booth, T. Stauber, et al., Fine structure constant defines visual transparency of graphene, Science 320 (2008) 1308-1308.
[16] B.C. Brodie, On the atomic weight of graphite, Philos. Trans. R. Soc. London 149 (1859) 249–259.
[17] L. Staudenmaier, Verfahren zur darstellung der graphitsäure, Berichte Der Dtsch. Chem. Gesellschaft 31 (1898) 1481–1487.
[18] S. William, J.R. Hummers, R.E. Offeman, Preparation of graphitic oxide, J. Am. Chem. Soc. 80 (1958) 1339-1339.
[19] C. Mattevi, E. Goki, A. Stefano, M. Steve, K.A. Mkhoyan, O. Celik, et al., Evolution of electrical, chemical, and structural properties of transparent and conducting chemically derived graphene thin films, Adv. Funct. Mater. 19 (2009) 2577–2583.
[20] S.J.R. Prabakar, Y.H. Hwang, E.G. Bae, D.K. Lee, M. Pyo, Graphene oxide as a corrosion inhibitor for the aluminum current collector in lithium ion batteries, Carbon 52 (2013) 128–136.
[21] Y.S. Dedkov, M. Fonin, C. Laubschat, A possible source of spin-polarized electrons: the inert graphene/Ni(111) System, Appl. Phys. Lett. 92 (2008) 052506.
[22] L. Lin, H. Wu, S.J. Green, J. Crompton, S. Zhang, D.W. Horsell, Formation of tunable graphene oxide coating with high adhesion, J. Chem. Soc. Faraday Trans. 18 (7) (2016) 5086–5090.
[23] I.K. Moon, J.I. Kim, H. Lee, K. Hur, W.C. Kim, H. Lee, 2D graphene oxide nanosheets as an adhesive over-coating layer for flexible transparent conductive electrodes, Sci. Rep. 3 (2013) 1112.
[24] Z.J. Fan, W. Kai, J. Yan, T. Wei, L.J. Zhi, J. Feng, Y.M. Ren, L.P. Song, F. Wei, Facile synthesis of graphene nanosheets via Fe reduction of exfoliated graphite oxide, ACS Nano 5 (2011) 191.
[25] K. Rhowmik, A. Mukherjee, M.K. Mishra, G. De, Stable Ni Nanoparticle–reduced graphene oxide composites for the reduction of highly toxic aqueous Cr(VI) at room temperature, Langmuir 30 (2014) 3209.
[26] L. Lin, X. Zheng, S. Zhang, D.A. Allwood, Surface energy engineering in the solvothermal deoxidation of graphene oxide, Adv. Mater. Interfaces 1 (2014) 1300078.
[27] S. Hosseinia, H. Savaloni, M. Gholipour Shahrakic, Design and engineering of sculptured nano-structures for application in hydrophobicity, J. Ind. Eng. Chem. 45 (2017) 391–403.
[28] A.C. Ferrari, J.F. Robertson, Interpretation of Raman spectra of disordered and amorphous carbon, Phys. Rev. B61 (2000) 14095.
[29] D.A. Chen, H. Feng, J. Li, Graphene oxide: preparation, functionalization, and electrochemical applications, Chem. Rev. 112 (2012) 6027–6053.
[30] Y. Dongxing, A. Velamakanni, G. Bozoklu, S. Park, M. Stoller, R.D. Piner, et al., Chemical analysis of graphene oxide films after heat and chemical treatments by X-ray photoelectron and Micro-Raman spectroscopy, Carbon 47 (2009) 145–152.
[31] M.A. Pimenta, G. Dresselhaus, M.S. Dresselhaus, L.G. Cancado, A. Jorio, R. Saito, Studying disorder in graphite-based systems by Raman spectroscopy, J. Chem. Soc. Faraday Trans. 9 (2007) 1276–1290.
[32] M.S. Dresselhaus, G. Dresselhaus, M. Hofmann, Raman spectroscopy as a probe of graphene and carbon nanotubes, Philos. Trans. R. Soc. Lond. A 366 (2008) 231–236.
[33] A.C. Ferrari, Raman spectroscopy of graphene and graphite: disorder, electron–phonon coupling, doping and nonadiabatic effects, Solid State Commun. 143 (2007) 47–57.
[34] A. Gupta, G. Chen, P. Joshi, S. Tadigadapa, P.C. Eklund, Raman scattering from high-frequency phonons in supported n-graphene layer films, Nano Lett. 6 (2006) 2667–2673.
[35] C.B. Breslin, A.L. Rudd, Activation of pure Al in an indium-containing electrolyte—an electrochemical noise and impedance study, Corros. Sci. 42 (2000) 1023–1039.
[36] M. Keddam, C. Kuntz, H. Takenouti, D. Schustert, D. Zuili, Exfoliation corrosion of aluminium alloys examined by electrode impedance, Electrochim. Acta 42 (1997) 87–97.